Role of the oxygen partial pressure in the formation of composite Co–CoO nanoparticles by reactive aggregation

J. A. De Toro[†], J. P. Andrés, J. A. González, J. M. Riveiro
Instituto Regional de Investigación Científica Aplicada (IRICA) and Departamento de Física Aplicada, Universidad de Castilla–La Mancha, 13071 Ciudad Real, Spain.

M. Estrader, A. López–Ortega
Catalan Institute of Nanotechnology (ICN) and CIN2 and Universitat Autònoma de Barcelona, Campus UAB, E–08193 Bellaterra (Barcelona), Spain.

I. Tsiaoussis, N. Frangis
Solid State Physics Section, Department of Physics, Aristotle University of Thessaloniki, GR-54124 Thessaloniki, Greece.

J. Nogués
Institució Catalana de Recerca i Estudis Avançats (ICREA), Barcelona, Spain
Catalan Institute of Nanotechnology (ICN) and CIN2 and Universitat Autònoma de Barcelona, Campus UAB, E–08193 Bellaterra (Barcelona), Spain.

keywords: exchange bias, magnetic nanoparticles, cluster source, nanocomposite.

The magnetic properties of diluted films composed of nanocomposite Co–CoO nanoparticles (of ~8 nm diameter) dispersed in a Cu matrix have been investigated. The nanoparticles were formed in an aggregation chamber by sputtering at different Ar/O_2 partial pressures (0–0.015). The exchange bias properties appear to be insensitive to the amount of O_2 during their formation. However, the temperature dependence of the magnetization, M(T), exhibits two different contributions with relative intensities that correlate with the amount of O_2. The magnetic results imply that two types of particles are formed, nanocomposite Co–CoO (determining the exchange bias) and pure CoO, as confirmed by transmission electron microscopy observations. Importantly, as the O_2 partial pressure during the sputtering is raised the number of nanocomposite Co–CoO nanoparticles (exhibiting exchange bias properties) is reduced and, consequently, there is an increase in the relative amount of pure, antiferromagnetic CoO particles.

[†] Corresponding author's email: joseangel.toro@uclm.es

I. Introduction

Magnetic nanoparticles (NPs) are the subject of extensive research due to their rich phenomenology, strikingly different to their bulk counterparts, and to their ever increasing number of applications (Batlle and Labarta 2002; Lu et al 2007; Tartaj et al 2003; Willard et al 2004). The magnetic properties of ferromagnetic (FM) nanoparticles have been observed to be substantially modified when they are surrounded by an antiferromagnetic (AFM) shell due to exchange coupling (Nogues and Schuller 1999; Nogues et al 2005). In fact, this coupling, typically associated with "exchange–bias" (the horizontal shift of the hysteresis loop, H_E, after field cooling the sample through the Néel temperature of the AFM component in a FM–AFM heterostructure), was first discovered in surface oxidized Co nanoparticles half century ago (Meiklejohn and Bean 1956; Meiklejohn and Bean 1957). The topic has been recently enlivened by the discussion of the magnetically stabilizing effect produced by exchange coupling in core–shell FM–AFM nanoparticles, and its possible implications in high density storage media (Eftaxias and Trohidou 2005; Evans et al 2009; Skumryev et al 2003).

Since the exchange–bias field H_E is essentially determined by the FM–AFM interface area per unit volume of the ferromagnet (A_{FM-AFM}/V_{FM}) (Nogues and Schuller 1999; Nogues et al 2005) and the density of uncompensated spins in the AFM side of such interfaces [affecting J_{FM-AFM} (Fecioru-Morariu et al 2007; Takano et al 1997)], i.e., $H_E \propto J_{FM-AFM} \times A_{FM-AFM}/V_{FM}$, one may attempt to strengthen the exchange–bias effect by increasing both factors through the introduction of morphological disorder in the particles, i.e. moving from the usual core–shell structure to "composite" NPs comprising a disordered mixture of FM and AFM nanoscopic regions within the particle. Interestingly, while producing core–shell nanoparticles of transition metals is straightforward by simple passivation, producing composite nanoparticles is considerably harder. However, the technique of gas–phase aggregation (Binns et al 2005; Wegner et al 2006) is capable of such, more complex, synthesis by sputtering using an Ar/O_2 mixture (in contrast to using pure Ar), thus allowing the Co to partially oxidize while condensing to form the nanoparticles. We have recently shown the feasibility of this technique by growing films of composite Co–CoO nanoparticles (i.e., with no matrix) (De Toro et al 2009; Gonzalez et al 2009). Nevertheless, the magnetic properties of the films (Gonzalez et al 2009) were probably influenced by the "connectivity effect" (i.e., exchange interactions between CoO regions of different NPs) recently described by (Nogues et al 2006), therefore not reflecting the properties of the nanoparticles themselves, but those of the whole ensemble. To highlight the intrinsic properties of the nanoparticles, here we present the magnetic characterization of granular films comprising such Co–CoO composite particles highly dispersed (< 1% vol.) in a Cu matrix.

II. Experimental

Four different samples were prepared using different oxygen pressures in the condensation chamber, namely $P_{O2} = 0$ (S1), 6×10^{-4} (S2), 1×10^{-3} (S3) and 3×10^{-3} (S4) mbar. For all of them, the sputtering gas (Ar) pressure was kept at 0.2 mbar, the sputtering power at 60 W, and the aggregation length at 30 cm. The base pressure in the chamber was 2×10^{-6} mbar. The Cu matrix was co–deposited by rf–sputtering in the main deposition chamber at 5 Å/s. Moving a quartz crystal monitor in front of the sample holder, the particle deposition rate was measured to be about 0.2 Å/s at the beginning of each deposition. However, in order to obtain a sizeable magnetic signal, the deposition time had to be as long as 20 minutes, during which the nanoparticle deposition rate could not be monitored. Compositional microanalysis (EDAX) yielded values of about 2% at. for the Co concentration (close to the detection limit), thus confirming the diluted character of the samples. The magnetic characterization, as a function of temperature (5 -300 K) and applied field (up to 70 kOe), was done using Quantum Design SQUID magnetometry. Transmission electron microscopy (TEM) experiments were performed in a JEOL 2011 electron microscope, working at 200 kV, with a point resolution of 0.194 nm. TEM micrographs show that the oxygen pressure has no significant effect on the average particle size and that all the samples display a narrow particle size distribution with an average NP diameter of 8 nm. Note that in order to simplify the TEM experiments the grids have much larger nanoparticle densities than the diluted granular films used for the magnetic study.

III. Results and discussion

Figure 1 shows the hysteresis loops of the four samples measured at 10 K after cooling from room temperature in a field of 50 kOe. Note that in all cases the loops were measured up to 70 kOe and that the

diamagnetic contribution from the sample holder was subtracted. The curves have been normalized to allow a better comparison. Remarkably, the three samples grown in the presence of O_2 (S2–S4) have a very similar exchange bias field, H_E, and coercivity, H_C (see inset in Fig. 1). Moreover, the values H_E ~ 200 Oe and H_C ~400–500 Oe are surprisingly more than 50 times smaller than those obtained for composite nanoparticles films (i.e., without matrix) (Gonzalez et al 2009). On the other hand, the reference sample S1 (grown with nominally no oxygen), exhibits slightly larger H_E and H_C than samples S2–S4, proving that the nominally pure Co particles in this sample have in fact oxidized to some extent, thus forming a core–shell Co–CoO structure. The moderately low H_E and H_C values for S1 are consistent with the diluted character of these samples (Nogues et al 2006), in contrast to the large values obtained for dense nanoparticle films and powders (Nogues et al 2005).

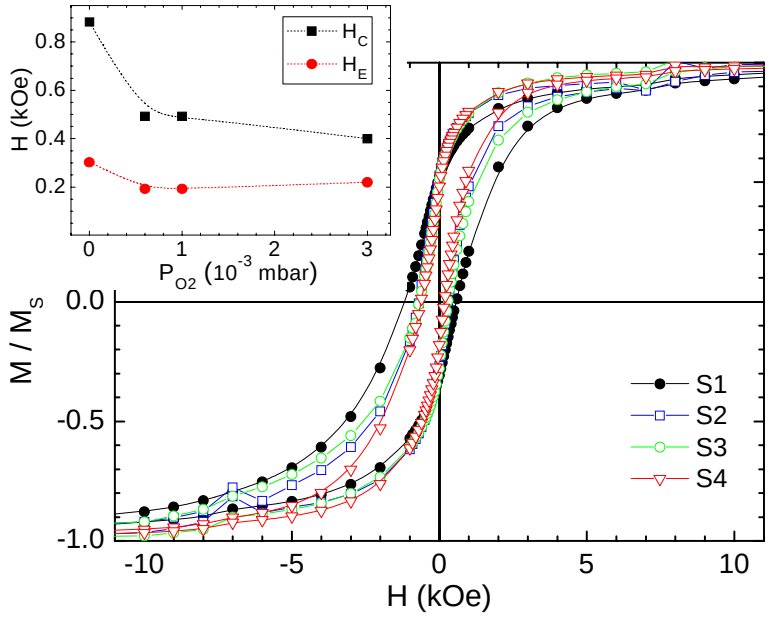

Fig. 1. Normalized hysteresis loops measured at 10 K after cooling from room temperature in a field of 50 kOe. The inset shows the exchange–bias and coercivity fields extracted from these loops. The lines are guides to the eye.

The results for samples S2–S4 confirm that isolated composite nanoparticles exhibit properties different to those of nanoparticulate dense films (without matrix) of the same nanoparticles. However, given their composite microstructure (with more AFM–FM interfaces, more disorder and possibly more uncompensated spins), the low values for H_E and H_C are somewhat unexpected. This result can probably be attributed to finite size effects in the antiferromagnetic regions (CoO) of the nanoparticles. Namely, each particle (of only 8 nm diameter) is probably composed of several AFM regions separated by FM regions. Consequently, most of these ultrafine AFM grains are exceedingly small to induce any bias, the anisotropy barrier being too low to render them thermally stable. This is due not only to the small size itself, but to its degrading influence on the ordering temperature and anisotropy of nanoscopic antiferromagnets, as reported both for films (Tang et al 2003) and nanoparticles (Sako et al 1996; Wang et al 2004). In highly concentrated samples, such as the composite NPs films studied by (Gonzalez et al 2009) exhibiting H_E values of several kOe, exchange coupling between neighbouring oxide regions of touching particles will tend to stabilize their AFM order and, thus, increase the exchange bias field. This mechanism was recently reported by (Nogues et al 2006), who found a striking three order of magnitude increase in the exchange bias field upon increasing the concentration of a granular film comprising Co–CoO core–shell nanoparticles with 1 nm thick shells. In core–shell nanoparticles with larger FM cores, the core could also help stabilizing the AFM shells through exchange interactions (Leighton et al 2002) or proximity effects (Golosovsky et al 2009). In our composite particles, instead of such FM core there are several remnants of non–oxidized Co. The magnetostatic energy of these small FM *fragments* would be correspondingly small, therefore having little effect on the stabilization of the AFM parts (Dobrynin et al 2005; Dobrynin et al 2007). In short, although the microstructure may be, in principle, adequate for the enhancement of exchange bias, finite size effects in such small nanoparticles dominate the magnetic properties.

Figure 2 presents the temperature dependence of the exchange bias (main panel) and coercive (inset) fields for the four samples studied. The onset temperature for exchange bias is the same, T_O = 170 K, for the tree samples with nanoparticles grown by reactive aggregation (S2, S3, S4), in agreement with the also similar values found for H_E. The core-shell sample (S1) displays a slightly higher onset temperature (T_O = 200 K). The low values found for T_O in all samples (as compared with T_N = 290 K in bulk CoO) are, in a sense, consistent with their moderate H_E and H_C (Nogues et al 2006). $T_2 \approx 170$ K implies a reasonable stability of the CoO AFM network in the composite nanoparticles (i.e., a moderate effective anisotropy), which, as discussed in (Nogues et al 2006), should translate in a moderate H_E. Regarding the coercive field, the inset of Fig. 2 shows the well known effect of coercivity enhancement associated to unidirectional exchange coupling, as the reduction of H_C with temperature reproduces that of H_E.

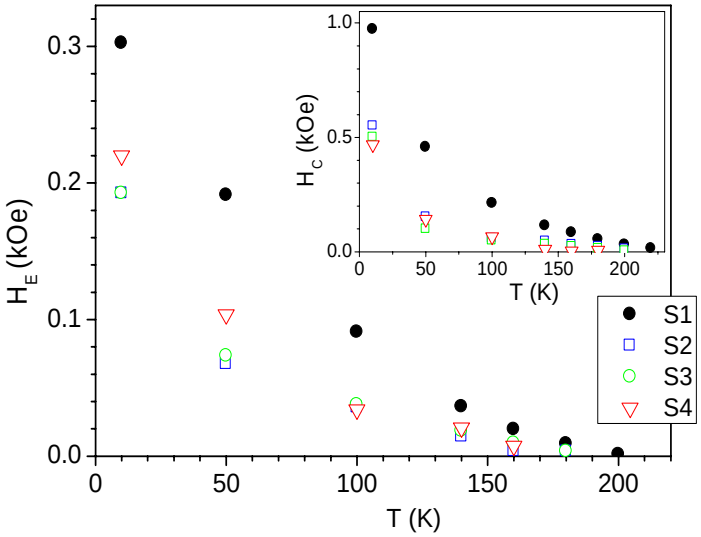

Fig. 2. Temperature dependence of the exchange bias field, H_E, (main panel) and coercivity, H_C (inset).

The fact that both the exchange bias field (inset of Fig. 1) and the onset temperature (Fig. 2) are virtually independent of the oxygen pressure in the aggregation chamber is rather intriguing. These results might be understood in a scenario where the main effect of an increasing O_2 pressure were the production of an increasingly large population of fully oxidized CoO particles (which due to their AFM character would not contribute to H_C and H_E), whereas the remaining particles, i.e., the composite Co–CoO NPs responsible for the observed exchange–bias effect, would not change significantly in structure.

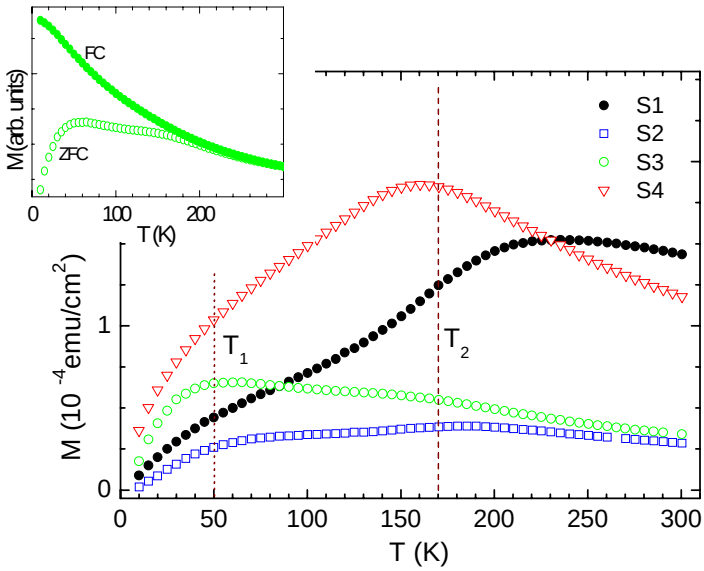

Fig. 3. Temperature dependence of the zero–field cooled (ZFC) and magnetization measured at H = 50 Oe. The inset gives an example of field cooled (FC) magnetization for one of the samples (S3). The dotted and dashed vertical lines signal the low (T_1) and high (T_2) temperature features, respectively, present in all samples comprising composite particles (S2, S3, S4).

In order to test this hypothesis, we have studied the thermal stability of the particles recording the temperature dependence of the magnetization, shown in Fig. 3. All curves were registered in H = 50 Oe upon heating from low temperature after cooling either in zero field (ZFC) or in the measuring field (FC). The magnetization of the FC curves increases monotonically at low temperatures, as exemplified in the inset for sample S3, which is characteristic of ideally isolated ensembles of magnetic nanoparticles with negligible interactions (Knobel et al 2008). Consequently, any influence of the "connectivity effect" (Nogues et al 2006) on the magnetic properties can be safely ruled out.

Remarkably, all the ZFC curves exhibit two clear components with different relative importance depending on the O_2 partial pressure: (i) a low temperature one at $T_1 \approx 50$ K, and (ii) a second feature at $T_2 \approx 170$ K (except in the reference sample, at 240 K). The two components can be ascribed to the blocking temperatures of the anticipated pure CoO and composite Co–CoO particles, respectively. In samples S2-S4 the second peak temperature, T_2, is the same as their exchange bias onset temperature. This coincidence, often observed in small heterostructured FM-AFM particles (Normile et al 2006; Nogués et al 2006), confirms that such maxima corresponds to the blocking temperature of composite nanoparticles comprising FM regions (metallic Co). It means that the stability of such regions is not determined by their size, but rather by the effective anisotropy contribution introduced by their exchange coupling to AFM regions (CoO) within the particle, which vanishes at $T_O = T_2 = 170$ K. Without this coupling, the ultrafine non-oxidized regions in the particles would block at lower temperatures. Regarding the core-shell reference sample (S1), its onset temperature is slightly higher (To ~ 200 K), but still lower than the blocking temperature (240 K). This can be understood in terms of the expected larger size of the Co cores in these particles (compared to the Co regions in the composite NPs), which would render them stable even when the exchange bias anisotropy contribution disappears.

Therefore, the data in Fig. 3 suggest that the varying oxygen pressure conditions do not result in homogeneous changes in the degree of oxidation of the particles, but only affect the relative fractions of composite Co–CoO and CoO particles, without changing significantly the nature of the two types of particles (e.g., the blocking temperatures remain virtually unaffected). Moreover, the samples with a higher magnetization (less oxidized) have a smaller low temperature component (less CoO), showing only a smooth hump at T_1. Conversely, the samples with lower magnetization (namely S2 and S3), thus probably with a higher oxide content, display clearly larger low temperature features (i.e., more CoO). Consistently, the reference sample (core–shell structured) has both a different blocking temperature (240 K) for the Co–CoO particles and a different exchange–bias field (300 Oe) with respect to the other three samples. Note that sample S1 also exhibits a smooth hump at low temperature revealing the presence of a small fraction of CoO particles.

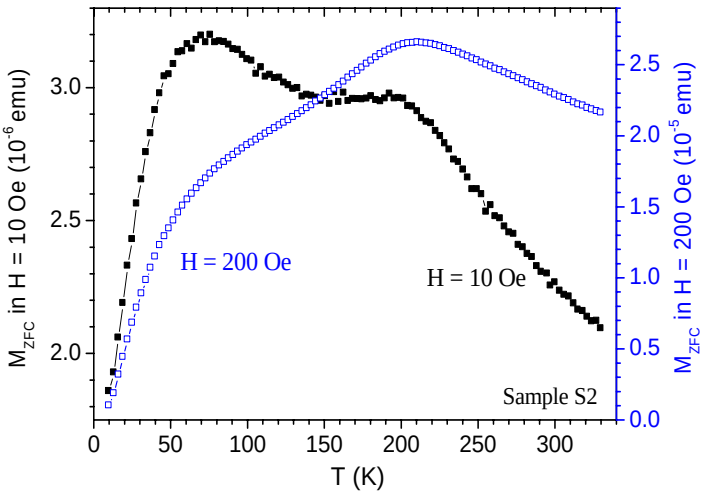

Fig. 4. Example (sample S2) of the effect of the measuring field (H = 10 Oe vs. 200 Oe) on the relative weight of the two components of the zero-field cooled magnetization curves.

The study of the ZFC magnetization curves measured in different applied fields supports, in its turn, the above ascription of the two components. Figure 4 illustrates the variation of their relative weight for sample S2 (a similar behaviour was observed in the other samples). The intensity of the peak at T_2 is smaller than that at T_1 when the curve is measured at low fields (as in H = 10 Oe in Figure 4), but increasing fields causes them to level and eventually make the second peak larger than the first feature.

This result can be well accounted for within our model: at low fields the magnetization of the majority AFM CoO particles (measured at T_1) is larger than that of the minority composite particles (measured at T_2), but increasing fields are expected to cause the susceptibility of the FM regions in the composite particles to increase sharply while that of the AFM particles remains constant, which explains why the second feature in the ZFC curves surpasses the low temperature one. Note that the ZFC curves are measured after demagnetizing at high temperature and, therefore, the magnetic response of the Co regions is given by the initial magnetization curve of a ferromagnet, which usually starts at small fields with a reversible stage characterized by a low magnetic susceptibility followed by a high susceptibility irreversible response at larger fields (Cullity and Graham 2009), thus supporting the above explanation.

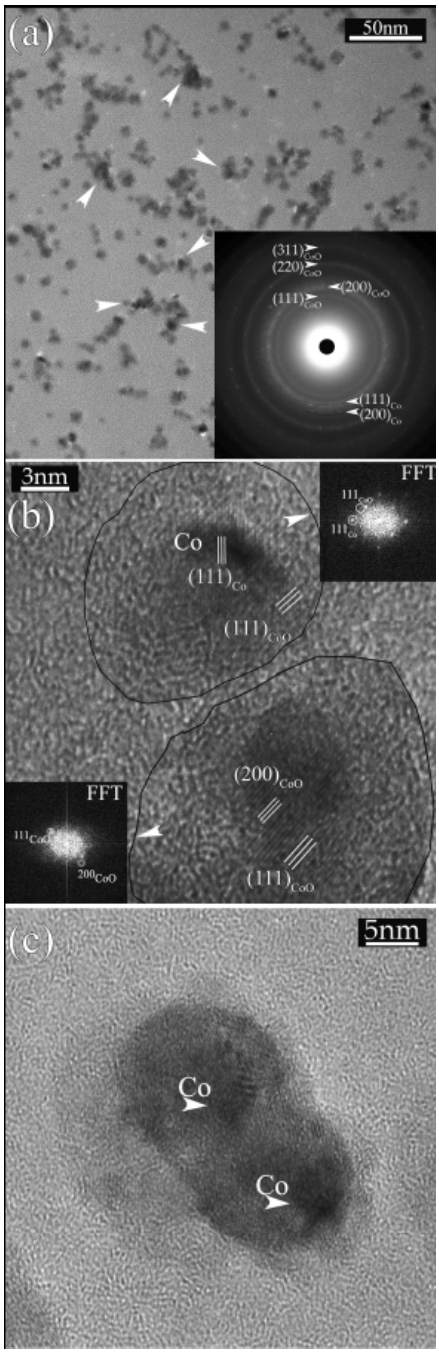

Fig. 5. TEM study for sample S2; (a) Low magnification TEM image. The arrows point to the nanoparticles with non-homogeneous contrast. Shown in the inset is the selective area diffraction of the same area. The different rings are indexed according to CoO and fcc-Co. (b) High resolution TEM image of two particles where the planes of the main crystallites are shown. The top and bottom insets correspond to the fast Fourier transforms (FFT) of the two particles. (c) High resolution TEM image of a nanocompostite Co-CoO particle where the Co crystallites are highlighted by arrows.

From the structural point of view, the analysis of the XRD patterns on analogous samples (Gonzalez et al 2009) evidences that the samples are mostly composed of CoO and that the amount of CoO increases for larger O_2 partial pressures. The TEM analysis for sample S2 further confirms the major presence of CoO in the samples. As can be seen from the low magnification image, the nanoparticles exhibit two different types of contrast (Fig. 5a), where most of the particles have an homogeneous contrast (corresponding to CoO) while some have a non-homegenous contrast (Co-CoO particles, see arrows in Fig. 5) Similarly, in the selective area diffraction pattern (inset in Fig. 5a), the CoO rings are more intense than the Co ones. Moreover, the simultaneous presence of pure CoO and Co-CoO composite nanoparticles can be unambiguously observed in Fig. 5b, which shows a fully oxidized particle (bottom - note that the FFT shows no evidence of Co) and a Co-CoO one (top -note the clear Co(111) spot in the FFT). Further, the high resolution TEM images also demonstrate the composite character of the nanoparticles, i.e., composed simultaneously of Co (marked by arrows) and CoO crystallites (see Fig. 5c).

Notably, no traces of other cobalt oxides were found, as expected from the scarce amount of available oxygen (manifested in the presence of a remaining fraction of particles containing non–oxidized Co in all the samples) and the fact that CoO is the least oxygen-consuming oxide. Moreover, this result is consistent with a previous study on reactive sputtering of cobalt (De Toro et al 2006), where no oxides other than CoO were detected as long as there remained a fraction of metallic Co (even if marginally small). Further, the conventional shape of the loops (as opposed to “double-loop” type loops) rules out any contribution to the hysteretic response from the pure CoO AFM nanoparticles, which have been reported to show FM–like hysteresis loops in some cases (Morup et al 2007; Nogues et al 2005), and therefore do not influence the exchange bias results. Interestingly, taking an average diameter of 8 nm for the CoO nanoparticles, a blocking temperature of $T_1 = 50$ K leads to an effective uniaxial anisotropy of 6.3×10^4 J/m^3, a value well within the rather wide range suggested in the literature (Kanamori 1957; Moran 1995). Assuming that the fully oxidized CoO particles correspond to the smallest nanoparticles in the distribution (more unlikely to prevent the oxidation of inner FM regions during and after the aggregation stage) would lead to larger values for the inferred effective anisotropy.

In summary, we have presented results on the magnetic properties of composite Co–CoO nanoparticles comprising a mixture of Co and CoO regions formed during the reactive aggregation of the particles using Ar/O_2 mixtures. The nanoparticles were dispersed to a low concentration in a Cu matrix to avoid connectivity effects in the studied exchange coupling effect, which yielded relatively low values for the exchange–bias field. The temperature dependence of the magnetization reveals the presence of two different types of particles, oxide (CoO) NPs and composite Co–CoO particles, with the same characteristics (such as blocking temperature and exchange bias field) regardless of the oxygen pressure in the condensation chamber, which only affects their relative population.

IV. Acknowledgments

We thank M. Rivera and E. Prado for their assistance in the synthesis of the samples, and O. Crisan for his help with the TEM characterization. We acknowledge financial support from the Consejería de Educación y Ciencia de Castilla-La Mancha (PAI08–0203–1207), the Generalitat de Catalunya (2009SGR1292) and the Consejo Interministerial de Ciencia y Tecnología (CICYT – MAT2008–01158/NAN and MAT2010-20616-C02).

References

Batlle X, Labarta A (2002): Finite-size effects in fine particles: magnetic and transport properties. Journal of Physics D-Applied Physics 35:R15-R42.

Binns C, Trohidou KN, Bansmann J, Baker SH, Blackman JA, Bucher JP, Kechrakos D, Kleibert A, Louch S, Meiwes-Broer KH, Pastor GM, Perez A, Xie Y (2005): The behaviour of nanostructured magnetic materials produced by depositing gas-phase nanoparticles. Journal of Physics D-Applied Physics 38:R357-R379.

Cullity BD, Graham CD (2009): Introduction to magnetic materials, 2nd edn., John Wiley & sons, inc.

De Toro JA, Andres JP, Gonzalez JA, Muniz P, Munoz T, Normile PS, Riveiro JM (2006): Exchange bias and nanoparticle magnetic stability in Co-CoO composites. Physical Review B 73:094449.

De Toro JA, Andres JP, Gonzalez JA, Muniz P, Riveiro JM (2009): The oxidation of metal-capped Co cluster films under ambient conditions. Nanotechnology 20:085710.

Dobrynin AN, Ievlev DN, Temst K, Lievens P, Margueritat J, Gonzalo J, Afonso CN, Zhou SQ, Vantomme A, Piscopiello E, Van Tendeloo G (2005): Critical size for exchange bias in ferromagnetic-antiferromagnetic particles. Applied Physics Letters 87:012501.

Dobrynin AN, Temst K, Lievens P, Margueritat J, Gonzalo J, Afonso CN, Piscopiello E, Van Tendeloo G (2007): Observation of Co/CoO nanoparticles below the critical size for exchange bias. Journal of Applied Physics 101:113913.

Eftaxias E, Trohidou KN (2005): Numerical study of the exchange bias effects in magnetic nanoparticles with core/shell morphology. Physical Review B 71:134406.

Evans RFL, Yanes R, Mryasov O, Chantrell RW, Chubykalo-Fesenko O (2009): On beating the superparamagnetic limit with exchange bias. Europhys. Lett. 88:57004.

Fecioru-Morariu M, Ali SR, Papusoi C, Sperlich M, Guntherodt G (2007): Effects of cu dilution in IrMn on the exchange bias of CoFe/IrMn bilayers. Physical Review Letters 99:097206.

Golosovsky IV, Salazar-Alvarez G, Lopez-Ortega A, Gonzalez MA, Sort J, Estrader M, Surinach S, Baro MD, Nogues J (2009): Magnetic Proximity Effect Features in Antiferromagnetic/Ferrimagnetic Core-Shell Nanoparticles. Physical Review Letters 102:247201.

Gonzalez JA, Andres JP, De Toro JA, Muniz P, Munoz T, Crisan O, Binns C, Riveiro JM (2009): Co-CoO nanoparticles prepared by reactive gas-phase aggregation. Journal of Nanoparticle Research 11:2105-2111.

Kanamori J (1957): Theory of the magnetic properties of ferrous and cobaltous oxides. Progress of Theoretical Physics 17:177-222.

Knobel M, Nunes WC, Socolovsky LM, De Biasi E, Vargas JM, Denardin JC (2008): Superparamagnetism and other magnetic features in granular materials: A review on ideal and real systems. Journal of Nanoscience and Nanotechnology 8:2836-2857.

Leighton C, Suhl H, Pechan MJ, Compton R, Nogues J, Schuller IK (2002): Coercivity enhancement above the Neel temperature of an antiferromagnet/ferromagnet bilayer. Journal of Applied Physics 92:1483-1488.

Lu AH, Salabas EL, Schuth F (2007): Magnetic nanoparticles: Synthesis, protection, functionalization, and application. Angewandte Chemie-International Edition 46:1222-1244.

Meiklejohn WH, Bean CP (1956): New Magnetic Anisotropy. Physical Review 102:1413-1414.

Meiklejohn WH, Bean CP (1957): New Magnetic Anisotropy. Physical Review 105:904-913.

Moran TJ (1995): Exchange coupling at ferromagnet-antiferromagnet interfaces, University of California San Diego.

Morup S, Madsen DE, Frandsen C, Bahl CRH, Hansen MF (2007): Experimental and theoretical studies of nanoparticles of antiferromagnetic materials. Journal of Physics-Condensed Matter 19:213202.

Nogues J, Schuller IK (1999): Exchange bias. Journal of Magnetism and Magnetic Materials 192:203-232.

Nogues J, Skumryev V, Sort J, Stoyanov S, Givord D (2006): Shell-driven magnetic stability in core-shell nanoparticles. Physical Review Letters 97:157203.

Nogues J, Sort J, Langlais V, Skumryev V, Surinach S, Munoz JS, Baro MD (2005): Exchange bias in nanostructures. Physics Reports-Review Section of Physics Letters 422:65-117.

Sako S, Ohshima K, Sakai M, Bandow S (1996): Magnetic property of CoO ultrafine particle. Surface Review and Letters 3:109-113.

Skumryev V, Stoyanov S, Zhang Y, Hadjipanayis G, Givord D, Nogues J (2003): Beating the superparamagnetic limit with exchange bias. Nature 423:850-853.

Takano K, Kodama RH, Berkowitz AE, Cao W, Thomas G (1997): Interfacial uncompensated antiferromagnetic spins: Role in unidirectional anisotropy in polycrystalline Ni81Fe19/CoO bilayers. Physical Review Letters 79:1130-1133.

Tang YJ, Smith DJ, Zink BL, Hellman F, Berkowitz AE (2003): Finite size effects on the moment and ordering temperature in antiferromagnetic CoO layers. Physical Review B 67:054408.

Tartaj P, Morales MD, Veintemillas-Verdaguer S, Gonzalez-Carreno T, Serna CJ (2003): The preparation of magnetic nanoparticles for applications in biomedicine. Journal of Physics D-Applied Physics 36:R182-R197.

Wang L, Vu K, Navrotsky A, Stevens R, Woodfield BF, Boerio-Goates J (2004): Calorimetric study: Surface energetics and the magnetic transition in nanocrystalline CoO. Chemistry of Materials 16:5394-5400.

Wegner K, Piseri P, Tafreshi HV, Milani P (2006): Cluster beam deposition: a tool for nanoscale science and technology. Journal of Physics D-Applied Physics 39:R439-R459.

Willard MA, Kurihara LK, Carpenter EE, Calvin S, Harris VG (2004): Chemically prepared magnetic nanoparticles. International Materials Reviews 49:125-170.